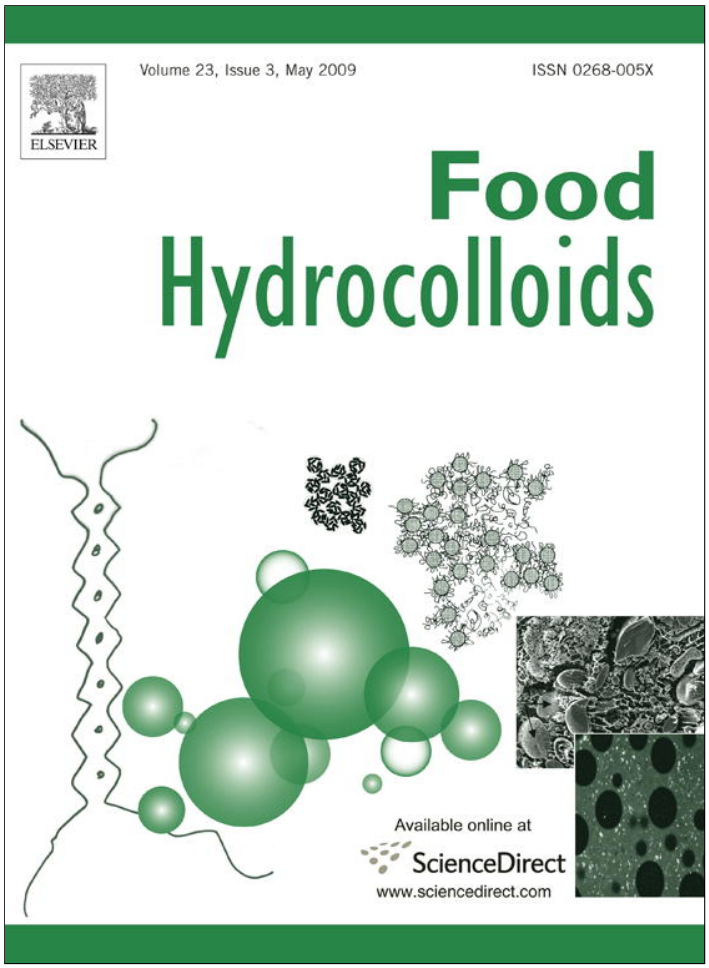

Food Hydrocolloids 23 (2009) 964–972

Contents lists available at ScienceDirect

Food Hydrocolloids

journal homepage: www.elsevier.com/locate/foodhyd

Linear viscoelasticity and microstructure of heat-induced crayfish protein isolate gels

Alberto Romero [a], Felipe Cordobés [a], Mª Cecilia Puppo [b], Álvaro Villanueva [c], Justo Pedroche [c], Antonio Guerrero [a,*]

[a] Departamento de Ingeniería Química, Universidad de Sevilla, Facultad de Química, C/P. García González 1, 41012 Sevilla, Spain
[b] Centro de Investigación y Desarrollo en Criotecnología de Alimentos (CIDCA), CONICET, Universidad Nacional de La Plata, 47 y 116, 1900 La Plata, Argentina
[c] Instituto de la Grasa (CSIC), Av. Padre García Tejero 4, 41012 Sevilla, Spain

ARTICLE INFO

Article history:
Received 18 December 2007
Accepted 7 July 2008

Keywords:
Crayfish
Protein gelation
Rheology
Linear viscoelasticity
Microstructure
SEM

ABSTRACT

Linear dynamic viscoelastic properties have been used to evaluate the influence of heat processing on the microstructure of crayfish protein isolate (CFPI) in order to explore the potentials of crayfish in the production of surimi-like gel products. CFPI dispersions have been subjected to a temperature cycle that consisted of a constant heating rate temperature ramp and a rapid cooling step, following the transitions taking place in the system through the evolution of G' and G'', under different CFPI concentrations and pH values. The influence of CFPI concentration and pH on linear viscoelasticity functions of CFPI aqueous systems before and after thermal processing has also been analysed. Occurrence of a gel-like behaviour has been found for CFPI dispersions. The mechanical spectra of CFPI gels have revealed a remarkable enhancement in gel strength by thermal processing. An apparent gel network enhancement has also been found by increasing the CFPI content or reducing the pH, excepting at the isoelectric point. The strong dependence of microstructure on pH found for thermally processed CFPI gels has been confirmed by Electron Microscopy.

1. Introduction

Crayfish flour from red crayfish (*Procambarus Clarkii*) is a fairly attractive source of high quality protein (ca. 64 wt%) that may be obtained as a by-product in the red crayfish industry, which typically produces important crayfish surpluses. The potential of crayfish protein as a functional ingredient in food products has been recently explored (Cremades, 2004) although its application as a source of a low-fat, high-protein processed food has not yet been fully investigated.

Three major groups of proteins are found in crustaceans: water-soluble sarcoplasmic proteins (about 30 wt%) that consist of albumins and lower amounts of myoglobin and enzymes; salt-soluble myofibillar proteins (60–70 wt%), composed of up to 20 distinct proteins, containing principally myosin, actin and less amount of tropomyosin and troponin (Suzuki, 1981); and insoluble stromal proteins which represent only between 3 and 10 wt% of total proteins.

It is currently recognized that sarcoplasmic proteins, which possess a relatively simple globular structure, have poor gelling ability and contribute very little to food texture (Xiong, 1997). Myofibrillar proteins have highly reactive surfaces once the protein is unfolded (denatured). During heating, the proteins unfold, exposing the reactive surfaces of neighbouring protein molecules, which then interact to form intermolecular bonds. When sufficient bonding occurs, a three-dimensional network is formed, resulting in a gel. Four main types of chemical bonds (hydrogen bonds, ionic linkages, hydrophobic interactions, and covalent bonds) are involved in gel formation. Furthermore, according to Smyth, O'Neill and Smith (1999) factors affecting the balance between these forces, for example pH, ionic strength and temperature, will alter the type of gel formed and its rheological properties.

With respect to meat processing, myosin is one of the most interesting proteins due to its excellent gelling and binding properties (Ziegler & Acton, 1984). Myosin is of major importance as a heat-gelling and water-binding constituent of fish muscle. Thus, the rheology of myosin sols and gels commands the interest of meat scientists (Egelandsdal, Fretheim, & Samejima, 1986). Myosin is a relatively large protein, with a molecular weight of 470 kDa (Bechtel, 1986) and is unusual in that it has both fibrous (long extended shape) and globular (spherical shape) properties. Most capable of gelling protein ingredients in foods, such as those derived from egg, milk, whey and soy, are globular proteins. These globular proteins may be found as monomers or combined forming

* Corresponding author. Tel.: +34 954557179; fax: +34 954556447.
E-mail address: aguerrero@us.es (A. Guerrero).

0268-005X/$ – see front matter © 2008 Elsevier Ltd. All rights reserved.
doi:10.1016/j.foodhyd.2008.07.008

up to hexamers, and may exhibit a wide range of molecular weights, between 15 and 360 kDa (Ludescher, 1996; Marcone et al., 1998) Each myosin molecule is composed of two 220-kDa heavy amino acid chains and two pairs of different light chains, ranging from 17 to 22 kDa (Lowey & Risby, 1971). The heavy chains interact to form two distinct domains: a pair of globular "heads" (S1) and a fibrous or elongated domain, the so-called "rod" (Lanier, Carvajal, & Yongsawatdigul, 2004).

Although actin does not form gels when heated, it is reported to have a synergistic role in the gelation of myofibrillar proteins (Ishioroshi, Samejima, Aire, & Yasui, 1980; Samejima, Ishioroshi, & Yasui, 1981; Yasui, Ishioroshi, & Samejima, 1982). The complex formed between actin and myosin seemed to behave as a cross-link between the rod portions of myosin molecules, and consequently increased the rigidity of the gel (Lanier et al., 2004).

The term gel is applied to a wide range of substances, which exhibit solid-like properties while a vast excess of solvent is present. Typically, biopolymer gels contain more than 90 wt% of water (Doublier, Launay, & Cuvelier, 1992). Such a peculiar behaviour arises from the formation of a three-dimensional structure, which extends throughout the whole systems where the continuous phase is entrapped within the network. Consequently, as has been found for most food gels, the system usually exhibits a complex viscoelastic behaviour, which can be subjected to rigorous investigation by rheological techniques, particularly those using small deformation such as Small Amplitude Oscillatory Shear measurements (Foegeding, 1989). In general, rheological measurements have been considered as an analytical tool to provide fundamental insights into the structural organization of food and play an important role in process design of food processing plants. Therefore, as has been recently emphasized, there exists a strong interest in the study of the rheological properties of food products, which has lasted for many years, with particular attention paid to linear dynamic viscoelastic properties that are strongly influenced by temperature, concentration and physical state of dispersion (Binsi, Shamasundar, & Dileep, 2007).

This work is part of a comprehensive study whose overall objective is to evaluate the potentials of red crayfish in the production of surimi-like gel products. This paper is focused on heat-induced gelation kinetics of CFPI aqueous dispersions that were analysed as a function of composition (pH and concentration) and processing variables by means of small amplitude oscillatory shear (SAOS), performed at constant frequency and heating rate.

2. Materials and methods

2.1. Materials

Crayfish flour (CF) was manufactured on a pilot-plant scale by ALFOCAN S.A. (Isla Mayor, Seville, Spain). Crayfish meat was separated from the exoskeleton by grinding and filtration leading to meat slurry formed by the whole body of crayfish excepting for the shell. This crayfish meat slurry was dried at 150–160 °C in a rotatory drum dryer, to obtain a low moisture crayfish powder. The flour supplied by ALFOCAN S.A. consisted of 64 wt% protein, 18 wt% lipids, 13 wt% ashes and 5 wt% moisture.

All general chemicals used were of analytical grade purchased from Sigma Chemical Company (St. Louis, MO, USA). Distilled water was used for the preparation of all solutions.

2.2. Methods

2.2.1. Preparation of crayfish protein isolate

Crayfish protein isolate (CFPI) was prepared from crayfish flour by solvent extraction of lipids, alkaline extraction of soluble proteins and isoelectric precipitation. Crayfish flour powder was sieved by using a 600 μm mesh and was then defatted by percolation and maceration process for two days with hexane at 30 °C. The flour was air-dried and stored at 4 °C until use. Defatted flour was dispersed in water (10% w/v) giving rise to a pH of 6.6 that was adjusted to pH 10.5 with 25% NaOH. The dispersion was stirred at room temperature for 4 h and centrifuged at 900 × *g* for 25 min at 4 °C in an RC5C Sorvall centrifuge (Sorvall Instruments, Wilmington, DE, USA). The supernatant was then adjusted with 6 N HCl to pH 3.4, which corresponds to the actual p*I* of crayfish protein system (Romero, Cordobés, Puppo, Guerrero, & Bengoechea, 2008), and centrifuged at 9000 × *g* for 10 min at 4 °C. The pellet was washed and resuspended with distilled water. The protein dispersion was freeze-dried in a Freeze Mivile 3 (VIRTIS, USA).

2.2.2. Chemical composition of crayfish flour protein isolate

CFPI, obtained according to the above described isolation procedure, consisted of 90.61 wt% protein, 0.96 wt% lipids, 3.98 wt% ashes and 4.45 wt% moisture.

The protein content was determined in quadruplicate as %N × 6.25 using a LECO CHNS-932 nitrogen micro analyzer (Leco Corporation, St. Joseph, MI, USA) (Etheridge, Pesti, & Foster, 1998). Lipid content was analysed by Soxhlet extraction. Moisture and ash content of the isolate was determined in quadruplicate by AOAC (1995) approved methods.

2.2.3. Determination of protein isoelectric point (pI) and solubility

For determination of the p*I*, aqueous flour dispersions (0.96 g protein/40 mL) were prepared and pH of different aliquots was adjusted with 6 N NaOH and 2 and 6 N HCl to alkaline and acid pHs. Percentages of soluble protein (calculated as protein content of supernatant × 100/weight of CFPI powder) were plotted vs. pH to determine the p*I*.

The solubility was determined in different buffers with water, SDS (sodium dodecyl sulphate) and SDS with a reducing agent as DTT (dithiothreitol) and the percentages of soluble protein in the supernatants were calculated as previously indicated.

2.2.4. Rheological measurements

Linear dynamic viscoelasticity measurements, including strain sweep, frequency sweep or temperature ramp tests, were performed in a controlled-strain rheometer (ARES) from TA Instruments (USA). Strain sweep tests were performed in order to delimitate the linear viscoelastic range. All the dynamic viscoelasticity frequency sweep measurements were carried out at a strain clearly lower than the critical value for linear viscoelasticity.

The temperature cycle was performed with three different steps:

–The first step consisted of a temperature ramp carried out at constant heating rate (1.5 °C/min) from 20 °C to 90 °C.
–After the first step, a sudden decrease (10 °C/min) in temperature from 90 to 20 °C was performed.
–Finally, an equilibration stage at the end of the temperature cycle was carried out.

To ensure a correct strain control, strain sweep tests were previously performed for different regions and samples to keep measurements within the linear response regime. Plate–plate geometry (25 mm) with rough surfaces was used, setting a gap between plates of 1 mm. All the samples were maintained in the sensor system for 10 min before running any rheological test. At least two replicates were performed for each rheological measurement.

2.2.5. Electron microscopy

Scanning electron microscopy (SEM) was used to evaluate the microstructure of the gels formed, following the same procedure used in a previous work for heat-set egg yolk gels (Cordobés, Partal, & Guerrero, 2004). Gel samples were immersed in 3% glutaraldehyde for 72 h and washed several times with distilled water and then post-fixed in 1% osmium tetroxide at 4 °C. SEM samples were rinsed for 1 h in distilled water before being dehydrated in a grade of ethanol series, 50, 70, 90 and 3 × 100 vol.% and dried at the critical point. Each dried sample was mounted on a bronze stub and coated with gold, the specimens being observed with a Philips XL-30 scanning electron microscope (The Netherlands).

3. Results and discussion

3.1. CFPI dispersions

3.1.1. Solubility curve as a function of pH

Fig. 1 displays the solubility curve for crayfish flour and crayfish protein isolate as a function of pH. Both protein systems display a typical behaviour between pH 2 and 8, showing a U-shaped solubility curve with a minimum in solubility for the isoelectric point. The minimum is reached at pH close to 4 which was near the value of 3.4 previously reported for the isoelectric point of crayfish flour obtained by particle charge measurements (Romero et al., 2008). The minimum is more pronounced for CFPI since most of the remaining soluble protein at the p*I* was removed during the isolation process. Both solubility curves also show a second minimum at pH close to 10 and a further increase with pH. A remarkable change in solubility behaviour takes place at the isoelectric point, as a consequence of the absence of electrostatic interactions, since the net surface charge of protein molecules is zero. Under such conditions, hydrophobically driven protein aggregation dominates, leading to a dramatic decrease in protein solubility, as may be seen in Fig. 1. These results suggest that the rod segments of myofibrillar proteins play an important role on protein solubility at alkaline pH. Thus, the p*I* for the rod segments of myosin is about 10.5 (Choi & Park, 2002; Lin & Park, 1998). Table 1 shows the percentage of soluble protein over the CFPI powder in different buffer solutions at pH 8. The value included in this table for the system without SDS is slightly lower than that shown in Fig. 1, since different buffer solutions were used. The use of SDS gives rise to the disruption of physical interactions such as electrostatic or hydrophobic interactions and hydrogen bonds, whereas the role of DTT is to break up covalent bonds such as inter- or intra-chain disulphide bonds. It may be deduced from Table 1 that the increase in solubility attributed to the use of SDS is much higher (~20%) than that corresponding to the use of DTT (~5%). It should be pointed out that 99% of total protein becomes soluble by using SDS + DTT buffer. Therefore, physical interactions are more important than chemical bonding although both of them participate in the CFPI powder.

Table 1
Soluble protein concentrations (wt%) over the CFPI powder in different buffer solutions at pH = 8

Buffer solution: pH 8	SDS buffer: pH 8	SDS + DTT buffer: pH 8
70.9	85.2	89.7

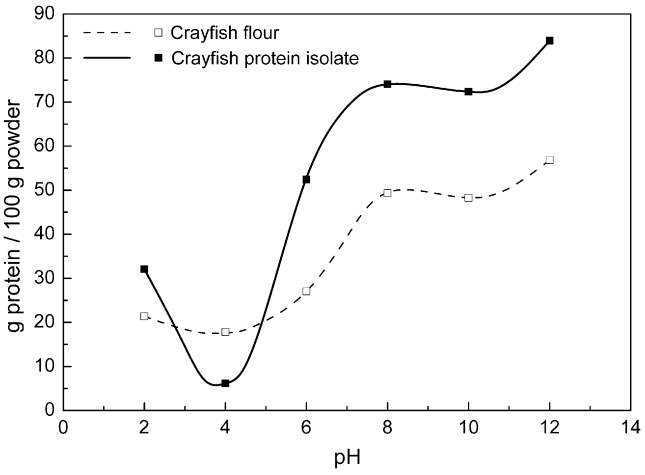

Fig. 1. Solubility curve for crayfish protein flour and crayfish protein isolate as a function of pH.

3.1.2. Influence of CFPI concentration

Fig. 2 shows the linear dynamic viscoelastic properties of CFPI aqueous dispersions prepared at pH 6 at different CFPI contents. All the dispersions studied exhibit a wide range of linear viscoelasticity as can be deduced from the sweep strain tests shown in Fig. 2a. The critical strain for the transition to the non-linear viscoelastic behaviour, calculated from the onset at which the stress is a non-linear function of strain, undergoes an increase with protein content. A remarkable increase in linear viscoelastic moduli takes place as CFPI concentration is raised from 6 to 15 wt% (i.e. two

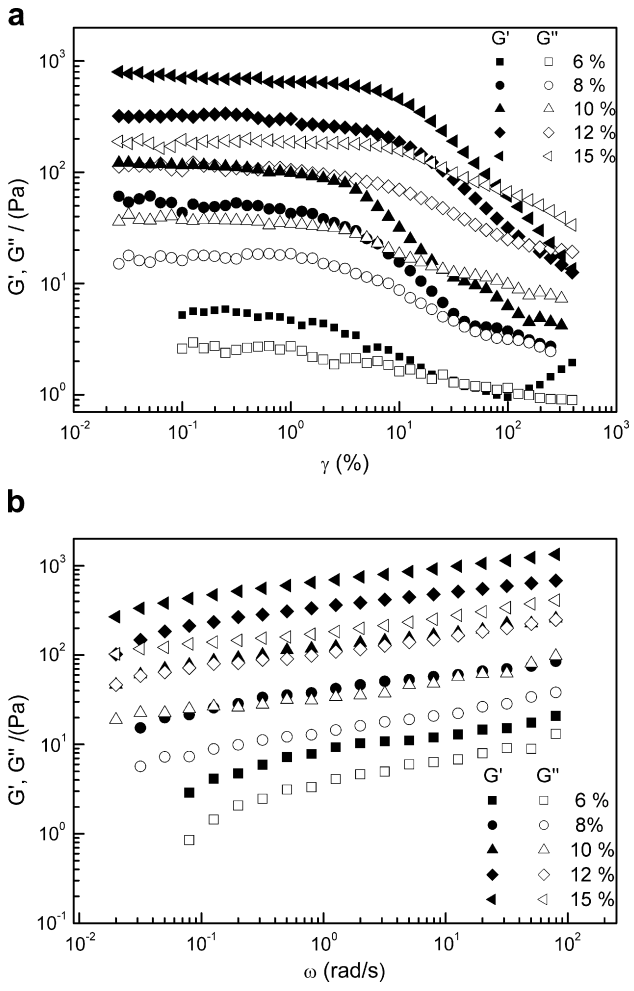

Fig. 2. Linear viscoelastic properties for CFPI dispersions at pH 6, as a function of concentration: (a) strain sweep tests and (b) frequency sweep measurements.

orders of magnitude for G'). However, all these dispersions show a similar viscoelastic response that corresponds to a gel-like behaviour, where G' is higher than G'', showing an almost parallel evolution within the whole frequency range. At the lowest CFPI concentration the behaviour is closer to that of a weak gel, but becomes stronger as the CFPI content is raised leading to a reduction in the slope of frequency–sweep curves for both viscoelastic functions. An increase in the elastic-predominant character of the dispersion with CFPI concentration may be also noticed in Fig. 2b.

3.1.3. Influence of pH

The results of strain–sweep and frequency–sweep tests are shown in Fig. 3 as a function of pH for aqueous dispersions containing 10 wt% CFPI. Fig. 3a shows a higher extension of the linear viscoelastic range for the alkaline dispersions (pH $\geq$ 8). It may also be noticed that the onset for non-linearity takes place in a different way for acid or alkaline dispersions. As may be observed in Fig. 3b, the highest values for G' and G'' and the smallest frequency dependence corresponds to pH 2, at which protein surfaces are positively charged. The behaviour is analogous to that previously described in Fig. 2b for pH 6. Near the isoelectric point, a remarkable reduction in G' and G'' is produced, giving rise to a very weak microstructure. In fact, the system is not completely stable at pH 3.4, and phase separation takes place eventually. An increase in pH above the p*I* generates negative charges on protein surfaces that lead to an increase in electrostatic interactions among protein molecules. In this way, the system recovers gel-like viscoelastic behaviour with a suitable level of stability against phase separation. A further increase in pH produces a continuous decrease in G' and G'', as well as a reduction in the gel-like character of the dispersion, leading to higher values of the loss tangent and to a tendency to a crossover point between G' and G'' in the low frequency regime.

3.2. Evolution along thermal processing

3.2.1. Influence of CFPI concentration

CFPI aqueous dispersions prepared at pH 6 were subjected to thermal treatment that consisted of a temperature ramp from 20 to 90 °C, performed at constant heating rate, and followed by a rapid decrease up to 20 °C. Fig. 4 shows the effect that this temperature cycle exerts on the linear dynamic viscoelastic properties obtained at constant frequency, at different CFPI concentrations. As may be observed, the thermomechanical profiles for all the concentrations are alike, always showing three different regions:

(i) At the beginning of the thermal treatment ($T < 45$ °C) a slight reduction in G', G'' and tan δ takes place. This stage involves an increase in mobility due to thermal agitation (i.e. the number of hydrogen bonds is significantly reduced), but protein aggregation is also possible. Thus, aggregation of the globular head regions of myofibrillar protein molecules has been reported for thermal processed meat, below 50 °C. The

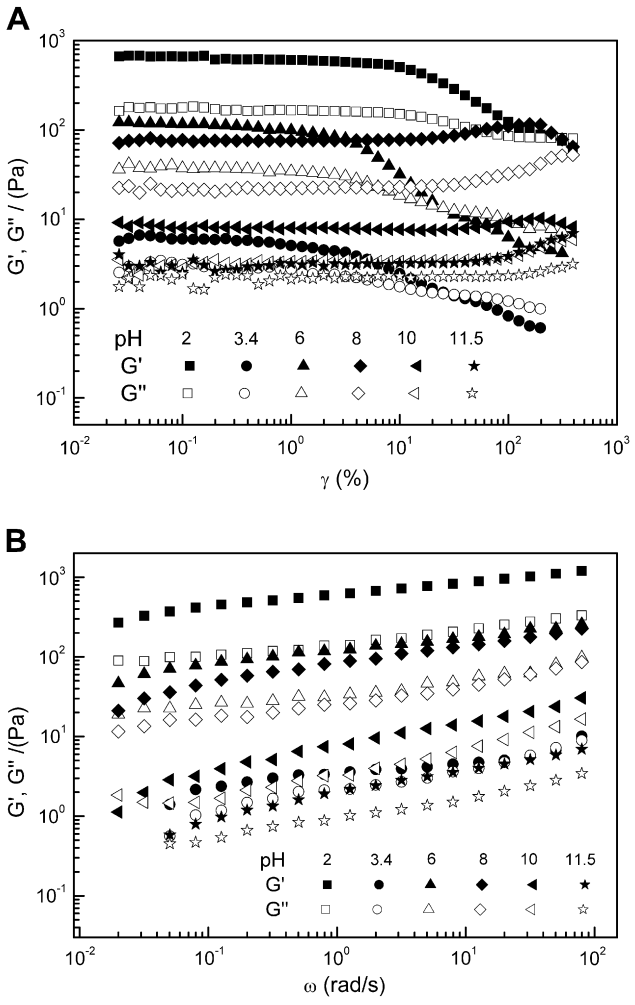

Fig. 3. Linear viscoelastic properties for dispersions containing 10 wt% CFPI, as a function of pH: (a) strain sweep tests and (b) frequency sweep measurements.

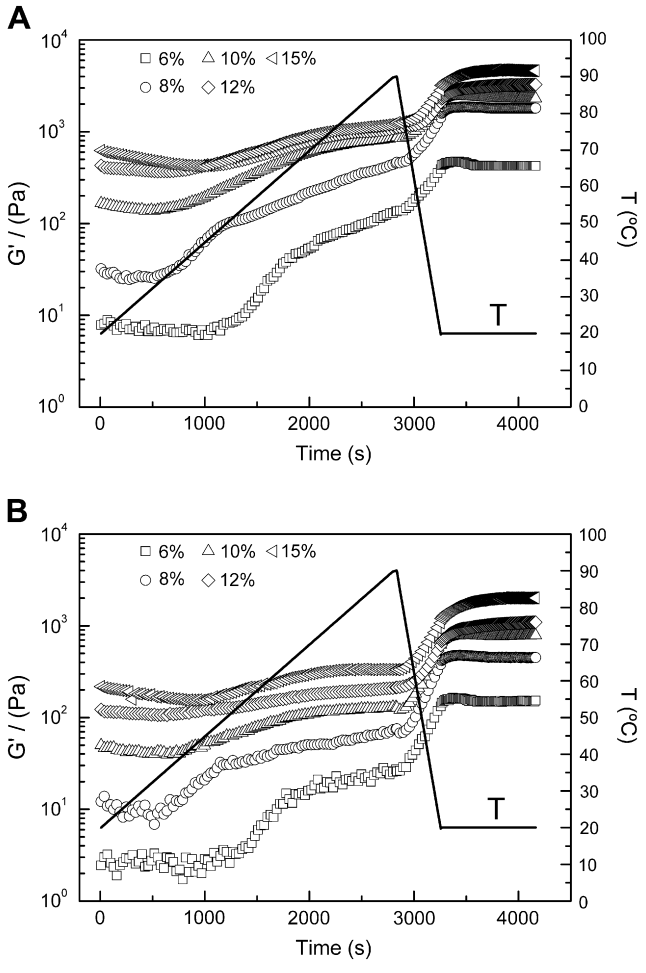

Fig. 4. Temperature ramp experiments performed at constant frequency, 0.63 rad/s, and constant heating rate, 1.5 °C/min, for CFPI dispersions as a function of concentration, (a) storage modulus and (b) loss modulus.

aggregation is thought to be dependent on the oxidation of sulfhydryl groups, predominantly found in the globular head segments, which show considerable reduction in the early temperature range of 30–50 °C (Acton & Dick, 1989; Ishioroshi et al., 1980; Samejima et al., 1981; Sano, Ohno, Osuka-Fuchino, Matsumato, & Tsuchiya, 1994). Some authors have attributed occurrence of a minimum in G' to denaturation of myosin molecules, indicating that α-helices in the tail portion start to unfold in the 30–40 °C region (Kim, Yongsawatdigul, & Thawornchinsombut, 2005; Yoon, Gunasekaran, & Park, 2004).

(ii) The first region is followed by an apparent increase in G' and G'' that show a tendency to asymptotic values at the end of the heating ramp. This is consistent with the results reported by Samejima et al. (1981) for heat-induced myosin gelation. The lost tangent is still decreasing in this region, but also tends to a constant value. This second stage must be associated with structural changes of the helical rod segments of myosin molecules which lead to network formation through cross-linking of these segments (Acton & Dick, 1989). Occurrence of a plateau in the gel modulus upon heat treatment has also been reported for myosin based protein gels (Ishioroshi, Samejima, & Yasui, 1981; Samejima et al., 1981; Yoon et al., 2004).

(iii) A further increase in both viscoelastic moduli occurs at the cooling region, giving rise to equilibrium values once the temperature of 20 °C is maintained. It may be pointed out that the enhancement in the viscous component is more relevant since the loss tangent also increases. Physical interactions, mainly hydrogen bonding, are responsible for this evolution. Hydrogen bonds between amino acids and water molecules, mainly formed during the cooling stage, can be important in the stabilization of the protein system. Moreover, hydrogen bonds also contribute to immobilize water into the hydrogel network (Lanier et al., 2004).

An increase in protein concentration produces a displacement of the results obtained at each region towards higher values. The temperature at the minimum in G' or G'', which corresponds to the end of the first stage, also tends to increase with CFPI concentration. Fig. 5 shows the values of the increments in G' and G'' obtained for each stage. As may be seen, $\Delta G'$ is always higher than $\Delta G''$. Stage 1 always leads to slightly negative values, being more significant at the highest concentration. The values for $\Delta G'$ at the second stage, where cross-linking among rod segments of myosin takes place, are much higher than $\Delta G''$, undergoing an increase with CFPI concentration. This evolution suggests an increase in the density of cross-linking with protein content. The values of $\Delta G'$ and $\Delta G''$ obtained along the cooling stage become more remarkable as protein concentration is raised.

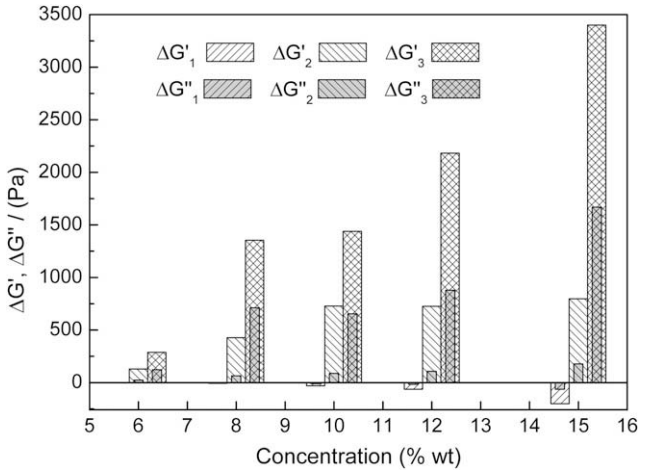

Fig. 5. Increments of linear viscoelastic functions for CFPI dispersions obtained from temperature ramp experiments at the three stages.

3.2.2. Influence of pH

The evolution of the viscoelastic moduli along the temperature cycle is displayed in Fig. 6 as a function of the pH value, for aqueous dispersions containing 10 wt% CFPI. All the protein systems show a similar profile as described above, excepting for the system processed at the p*I*, at which G' and G'' show the lowest initial values. It is worth mentioning that no first region takes place at the isoelectric point which reveals faster gelation kinetics. The first stage expands as the pH value increases, as may be observed in Fig. 6 and Table 2, which includes the values for the temperature at the minimum (T_m) in G' and the inflection point for the second stage (T_i). Moreover, a progressive delay of the whole temperature profile occurs with increasing pH as may be deduced from the displacement of the inflection temperature shown in Table 2. This evolution leads to slower gelation kinetics at the highest pH values. As a consequence, a longer second stage would be necessary under alkaline conditions, in order to reach a complete cross-linking process, at the experimental heating rate. The modifications produced on G' and G'' at the three stages are shown in Fig. 7, as

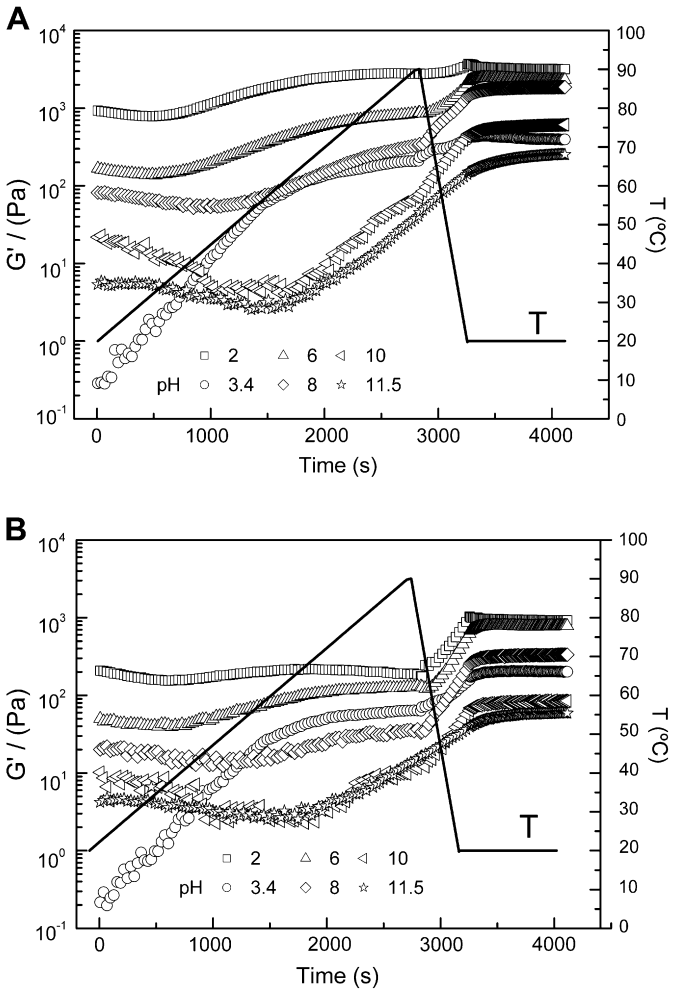

Fig. 6. Temperature ramp experiments performed at constant frequency, 0.63 rad/s, and constant heating rate, 1.5 °C/min, for CFPI dispersions as a function of pH, (a) storage modulus and (b) loss modulus.

Table 2
Values of T_m (temperature at which the storage modulus is minimum) and T_i (temperature at which an inflection point is observed) obtained from temperature ramps experiments for CFPI dispersions at different pH values

pH	2	3.4	6	8	10	11.5
T_m (°C)	32	20	32.8	38.8	56	58.3
T_i (°C)	57	60	65	78	85	90

a function of pH. As may be seen, the values for the $\Delta G'$ are generally higher than $\Delta G''$. The results obtained at the isoelectric point clearly differ from the general evolution. The highest modification produced by the thermal treatment corresponds to $\Delta G'_2$ at pH 2, at which little change in G'' is produced. These results suggest that cross-linking among protein rod segments is favoured at acidic pH below the p*I*. The thermally induced changes exerted on G' by this second stage undergo a remarkable reduction as the pH value increases and tends to be negligible at the highest pH values. In contrast, the effect of the second heating stage on G'' is generally very slight. The cooling region leads to a maximum value in $\Delta G'_3$ at neutral pH and a decrease in $\Delta G''_3$ with increasing pH (the isoelectric point is again an exception). A consequence of this behaviour is the remarkable effect of cooling on $\Delta G''_3$ that is even higher than $\Delta G'_3$ at low pH.

3.3. Thermal processed gels

3.3.1. Influence of CFPI concentration

Fig. 8 shows linear dynamic viscoelastic properties as a function of frequency for different CFPI concentrations. A gel-like behaviour is apparent for all the concentration studied, where a significant enhancement of the gel network is clearly induced by thermal processing. A similar effect has been recently reported by Binsi et al. (2007) for actomyosin from green mussels. Again, an increase in concentration leads to a remarkable displacement towards higher values in G' and G'', within the experimental frequency window. Fig. 9A and B show the evolution of some linear viscoelastic parameters with concentration, either for CFPI dispersions and gels (after thermal processing). The critical strain for linear viscoelasticity undergoes a continuous increase with CFPI content, which is quite independent of thermal treatment. Fig. 9A also displays the evolution of the slope of G' vs. frequency (n') as a function of concentration. No significant variation of n' takes place for the gels obtained after thermal processing at different CFPI contents, in

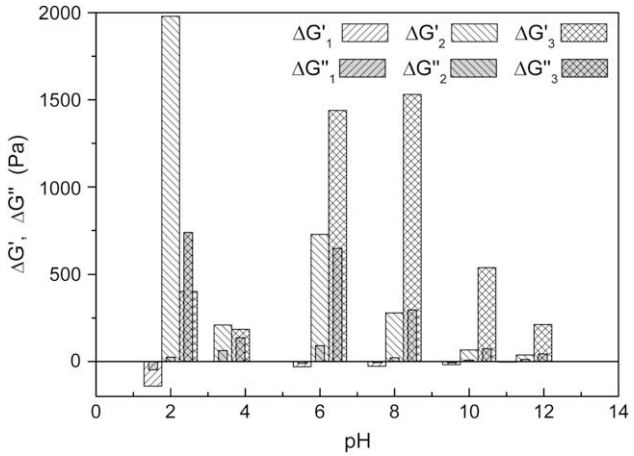

Fig. 7. Increments of linear viscoelastic functions for CFPI dispersions obtained from temperature ramp experiments at the three stages.

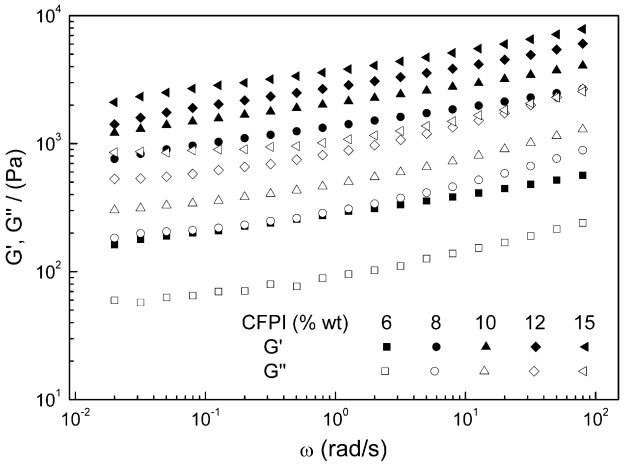

Fig. 8. Evolution of linear viscoelastic properties for CFPI gels as a function of concentration and frequency.

contrast to the results obtained before application of the temperature cycle, at which n' shows a decrease with concentration. However, it may be noticed that heat-processed gels always show smaller values for n' than unprocessed CFPI dispersions, which

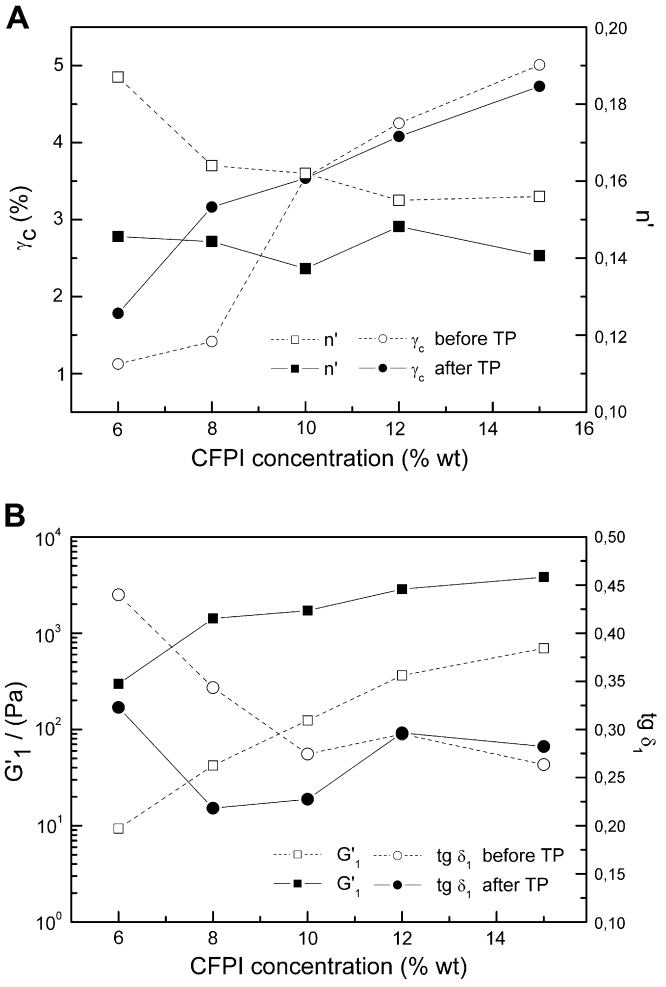

Fig. 9. Evolution of linear viscoelastic parameters for CFPI dispersions and gels at pH 6, as a function of concentration before and after thermal processing (TP): (a) critical strain for linear viscoelasticity and slope of storage modulus (n'), (b) storage modulus and loss tangent at 0.63 rad/s.

reveals the above mentioned heat-induced structural network enhancement. The storage modulus and loss tangent at 1 rad/s (G'_1 and tan δ_1) are plotted in Fig. 9B vs. CFPI concentration, before and after subjecting CFPI dispersions to thermal treatment. G'_1, which shows much higher values after thermal processing, undergoes a continuous increase with concentration. Moreover, tan δ_1 generally shows a decrease with concentration, being much lower after thermal processing excepting for the highest concentrations, at which processing does not yield significant differences.

3.3.2. Influence of pH

Fig. 10 plots linear dynamic viscoelastic properties vs. frequency for different pH values after thermal processing. All the systems exhibit gel-like behaviour, showing always a remarkable increase in gel strength over the corresponding unprocessed dispersion. The evolution of linear viscoelastic properties for CFPI gels with increasing pH is quite similar to that found for CFPI dispersions previously to thermal processing. Fig. 11a shows the evolution of the critical strain and the slope of G' with increasing pH. Two levels of critical strain may be noted in this figure for either CFPI dispersions or CFPI gels. At acidic conditions, no significant differences may be noted between γ_c for dispersions and gels ($\gamma_c < 9\%$), showing only a slight variation for different pH values with an almost imperceptible minimum at the p*I*. However, at alkaline conditions, at which the critical strain is higher than 45%, the increase in pH leads to a different evolution (an increase for unprocessed dispersions and a maximum at pH 10 for heat-induced gels), showing higher values for CFPI gels. At high pH the slope of G' exhibits different behaviour for unprocessed or thermal processed systems. For the latter systems, n' does not show any significant dependence on pH, whereas unprocessed dispersions show much higher values at high pH, when the protein solubility reaches a maximum value. This pH-induced weakening effect for CFPI dispersions may be also inferred from the evolution of G'_1 shown in Fig. 11b (i.e. G'_1 undergoes a reduction greater than two orders of magnitude). The behaviour at the isoelectric point deviates from the general tendency for dispersions and gel systems, showing low values for G'_1 and G''_1 (and high values of tan δ_1). Thermal processing leads to much higher values in G'_1 but the pH-induced weakening effect is less pronounced (G'_1 is only reduced about one order of magnitude). It may be also pointed out that the slowest gelation kinetics shown at the highest pH values would require a longer temperature processing time, as previously mentioned. These results are consistent with those obtained by

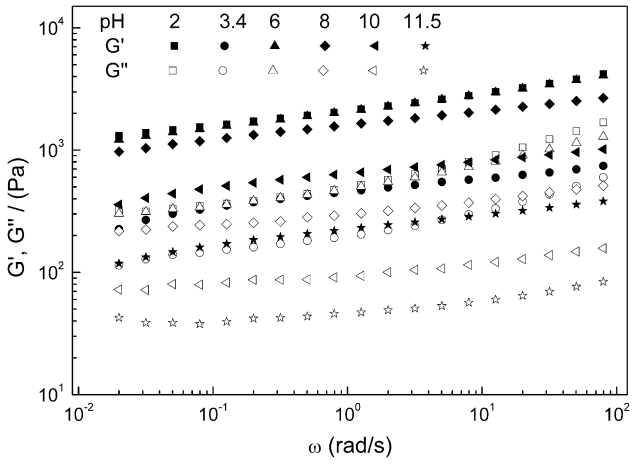

Fig. 10. Evolution of linear viscoelastic properties for CFPI gels as a function of pH and frequency.

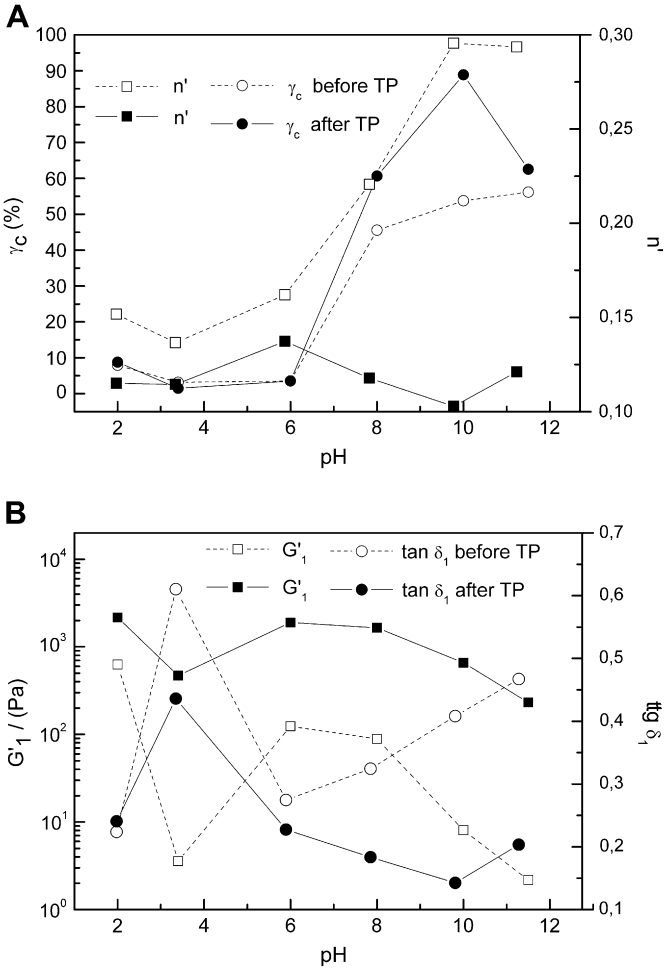

Fig. 11. Evolution of linear viscoelastic parameters for 10 wt% containing CFPI dispersions and gels, as a function of pH before and after thermal processing (TP): (a) critical strain for linear viscoelasticity and slope of storage modulus (n') and (b) storage modulus and loss tangent at 0.63 rad/s.

Samejima et al. (1981) and Ishioroshi et al. (1981) that reported maximum rigidity of heat-induced myosin gels at pH 6. The values for the loss tangent at alkaline pH after heat processing undergo an unexpected reduction that must be attributed to a higher development of physical interactions, taking place along the cooling stage.

Fig. 12 shows SEM images of heat-induced CFPI gels obtained at different pH values. As can be observed, a remarkable evolution of microstructure takes place with increasing pH. The image obtained at pH 2 (Fig. 12a) reveals occurrence of an extended network microstructure that seems to correspond to a system where cross-linking among protein rod segments prevail, as reported by Acton and Dick (1989). In fact, as suggested by Ishioroshi et al. (1981) the coiled coil α-helical tail of myosin molecules plays a critical role in the heat-induced gelation of myosin based systems. On the other hand, the rest of the SEM images show a sponge-like network with bead-like protein aggregates similar to the micrographs reported by Samejima et al. (1981) and Ishioroshi et al. (1981) for thermally induced gels of myosin and myosin sub-fragments. These aggregates are larger at the isoelectric point, in the absence of electrostatic interactions, where the gel-like characteristics are poorer. At alkaline pH, at which electrostatic interactions are predominant, protein aggregates are much smaller but the microstructure still retains some sponge-like appearance.

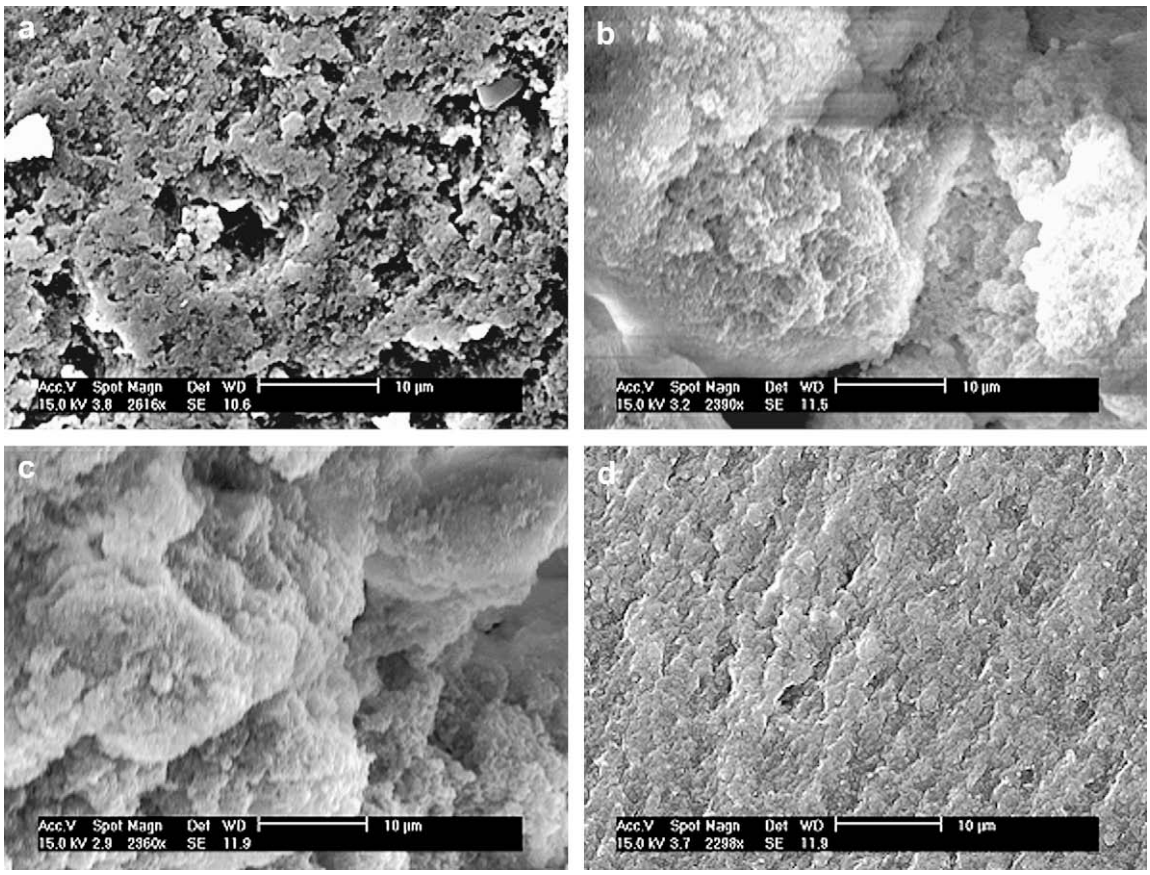

Fig. 12. SEM images for 10 wt% containing CFPI gels at different pH values: (a) pH = 2, (b) pH = 3.5, (c) pH = 6 and (d) pH = 10.

4. Concluding remarks

Linear dynamic viscoelastic properties of Crayfish Protein Isolate aqueous dispersions indicate occurrence of a gel-like behaviour. There is a tendency for CFPI dispersions to exhibit remarkable gelation properties even before the application of heat. This tendency could be connected with molecular changes brought about by the application of drum-drying to the CF protein concentrate used as the raw material for the isolation process. The drying process must have caused heavy denaturation and aggregation to CF proteins. In fact, this effect impairs emulsion ability of CF flour as previously reported (Romero et al., 2008; Romero, Cordobés, & Guerrero, 2008). Some small-sized protein aggregates and denatured protein molecules may remain among the isolate constituents after protein extraction, being responsible for the ability to form a gel-like network, even before thermal processing.

Dynamic viscoelastic measurements also reveal the ability to form network structures under thermal processing that leads to a remarkable enhancement in gel strength.

The evolution of linear viscoelastic properties also reveals an apparent enhancement of gel network microstructure for CFPI systems (either before or after thermal processing) by increasing CFPI concentration or by reducing pH, excepting at the isoelectric point. Both variables may modify the balance of forces to a high extent (particularly between electrostatic and hydrophobic interactions).

Electrostatic repulsive interactions play an important role in gelation kinetics. Thus, gelation kinetics is faster at the isoelectric point, when the balance of surface charges is zero, whereas the slowest kinetics corresponds to the highest pH values, at which the charge density at the protein surface is higher.

Scanning Electron Microscopy puts forward evidences of the strong dependence that pH exerts on microstructure of thermal processed CFPI gels, which is consistent with the results obtained from linear viscoelastic measurements performed either along thermal gelation and after thermal processing.

According to the results obtained, crayfish protein isolate prepared as a by-product from crayfish industry shows excellent gelling behaviour at suitable conditions of pH values (neutral or acidic, excepting for values closed to the p*I*). This fact confirms the potentials of red crayfish in the production of surimi-like gel products.

However, a modification of crayfish protein flour manufacture process, in order to minimize the impact of drying on CF protein denaturation and aggregation, should be highly beneficial, contributing to maintain its functional properties unaltered, which should lead to a significant improvement not only on CF emulsion ability, studied in a previous paper (Romero et al., 2008; Romero, Cordobes, & Guerrero, 2008), but also on the gelling behaviour of the protein isolate. Future work should be devoted to explore this alternative.

Acknowledgement

The authors wish to thank the Spanish "Ministerio de Educación y Ciencia" (MEC) for Mr. Romero's predoctoral fellowship (FPU grant). The authors also acknowledge financial support from MEC/FEDER under the project AGL2007-65709.

References

Acton, J. C., & Dick, R. L. (1989). In J. E. Kinsella, & W. G. Soucie (Eds.), *Functional roles of heat protein gelation in processed meat* (pp. 195–209). Champaign, IL: American Oil Chemists Society.

AOAC. (1995). *Official methods of analysis* (17th ed.). Washington, DC, USA: Association of Official Analytical Chemists.
Bechtel, P. J. (1986). In P. J. Bechtel (Ed.), *Muscle development and contractile proteins* (pp. 2–31). Orlando: F Academic Press.
Binsi, P. K., Shamasundar, B. A., & Dileep, A. O. (2007). Some physico-chemical, functional and rheological properties of actomyosin from green mussel (*Perna viridis*). *Food Research International, 39*, 992–1001.
Choi, Y. J., & Park, J. W. (2002). Acid-aided protein recovery from enzyme-rich Pacific Whtiting. *Journal of Food Science, 67*, 2962–2967.
Cordobés, F., Partal, P., & Guerrero, A. (2004). Rheology and microstructure of heat-induced egg yolk gels. *Rheologica Acta, 43*, 184–195.
Cremades, O. (2004). Caracterización y producción de carotenoproteínas de P. ClarkiiThesisUniversidad de Sevilla.
Doublier, J. L., Launay, B., & Cuvelier, G. (1992). In M. A. Rao, & J. F. Steffe (Eds.), *Viscoelastic properties of foods* (pp. 371–434). London: Elsevier Applied Science.
Egelandsdal, B., Fretheim, K., & Samejima, K. (1986). Dynamic rheological measurements on heat-induced myosin gels: effect of ionic strength, protein concentration and addition of adenosine triphosphate or pyrophosphate. *Journal of the Science of Food and Agriculture, 37*, 915–926.
Etheridge, R. D., Pesti, G. M., & Foster, E. H. (1998). A comparison of nitrogen values obtained utilizing the Kjeldahl nitrogen and Dumas combustion methodologies (Leco CNS 2000) on samples typical of an animal nutrition analytical laboratory. *Animal Feed Science and Technology, 73*, 21–28.
Foegeding, E. A. (1989). In J. E. Kinsella, & W. G. Soucie (Eds.), *Functional roles of heat protein gelation in processed meat* (pp. 185–194). Champaign, IL: American Oil Chemists Society.
Ishioroshi, M., Samejima, K., Aire, Y., & Yasui, T. (1980). Effect of blocking the myosin–actin interaction in heat-induced gelation of myosin in the presence of actin. *Agricultural and Biological Chemistry, 44*, 2185.
Ishioroshi, M., Samejima, K., & Yasui, T. (1981). Further studies on the roles of the head and tail regions of the myosin molecule in heat-induced gelation. *Journal of Food Science, 47*, 114–120.
Kim, Y. S., Yongsawatdigul, J., Park, J. W., & Thawornchinsombut, S. (2005). Characteristics of sarcoplasmic proteins and their interaction with myofibrillar proteins. *Journal of Food Biochemistry, 29*, 517–532.
Lanier, T., Carvajal, P., & Yongsawatdigul, J. (2004). In J. W. ParK (Ed.), *Surimi and Surimi Seafood* (pp. 435–489). Taylor & Francis.
Lin, T. M., & Park, J. W. (1998). Solubility of salmon myosin as affected by conformational changes at various ionic strengths and pH. *Journal of Food Science, 63*, 215–218.
Lowey, S., & Risby, D. (1971). Light chains from fast and slow muscle myosins. *Nature, 234*, 81–85.
Ludescher, R. D. (1996). Physical and chemical properties of amino acids and proteins. In Z. E. Sikorski (Ed.), *Chemical and functional properties and characterization* (pp. 23–70). New York: VCH.
Marcone, M. F., Kakuda, Y., & Yada, R. Y. (1998). Salt-soluble seed globulins of various dicotyledonous and monocotyledonous plants – I. Isolation/purification and characterization. *Food Chemistry, 62*, 27–47.
Romero, A., Cordobes, F., & Guerrero, A. (2008). Influence of pH on linear viscoelasticity and droplet size distribution of highly concentrated O/W crayfish flour-based emulsions. *Food Hydrocolloids*. doi:10.1016/j.foodhyd.2008.02.001.
Romero, A., Cordobes, F., Puppo, M. C., Guerrero, A., & Bengoechea, C. (2008). Rheology and droplet size distribution of emulsions stabilized by crayfish flour. *Food Hydrocolloids, 22*, 1033–1043.
Samejima, K., Ishioroshi, M., & Yasui, T. (1981). Relative roles of the head and tail portions of the molecule in heat-induced gelation of myosin. *Journal of Food Science, 46*, 1412–1418.
Sano, T., Ohno, T., Otsuka-Fuchino, H., Matsumoto, J. J., & Tsuchiya, T. (1994). Carp natural actomyosin: thermal denaturation mechanism. *Journal of Food Science, 59*, 1002–1008.
Smyth, A. B., O'Neill, E., & Smith, D. M. (1999). In R. I. Richardson, & G. C. Mead (Eds.), *Poultry meat science* (pp. 377–396). CAB International.
Suzuki, T. (1981). *Fish and krill processing techonology*. London: Applied Science Publishers.
Xiong, Y. L. (1997). In S. Damodaran, & A. Paraf (Eds.), *Food proteins: An overview, food proteins and their applications* (pp. 341–392). New York: Marcel Dekker.
Yasui, T., Ishioroshi, M., & Samejima, K. (1982). Effect of actomyosin on heat-induced gelation of myosin. *Agricultural and Biological Chemistry, 46*, 1049–1059.
Yoon, W. B., Gunasekaran, S., & Park, J. W. (2004). Characterization of thermo-rheological behavior of Alaska Pollock and Pacific Whiting Surimi. *Journal of Food Science, 69*, E338.
Ziegler, G. R., & Acton, J. C. (1984). Mechanisms of gel formation by proteins of muscle tissue. *Food Technology, 38*, 77.